# Two-stage orbital order and dynamical spin frustration in KCuF$_3$

James C. T. Lee[1], Shi Yuan[1], Siddhartha Lal[1,2†], Young Il Joe[1], Yu Gan[1], Serban Smadici[1], Ken Finkelstein[3], Yejun Feng[4], Andrivo Rusydi[5], Paul M. Goldbart[1,2], S. Lance Cooper[1]★ and Peter Abbamonte[1]★

The orbital degree of freedom is integral to many exotic phenomena in condensed matter, including colossal magnetoresistance and unconventional superconductivity. The standard model of orbital physics is the Kugel–Khomskii model[1], which first explained the symmetry of orbital and magnetic order in KCuF$_3$ and has since been applied to virtually all orbitally active materials[2]. Here we present Raman and X-ray scattering measurements showing that KCuF$_3$ exhibits a previously unidentified structural phase transition at $T = 50$ K, involving rotations of the CuF$_6$ octahedra. These rotations are quasi-ordered and exhibit glassy hysteresis, but serve to stabilize Néel spin order at $T = 39$ K. We propose an explanation for these effects by supplementing the Kugel–Khomskii model with a direct, orbital exchange term that is driven by a combination of electron–electron interactions and ligand distortions[3]. The effect of this term is to create a near degeneracy that dynamically frustrates the spin subsystem but is lifted at low temperature by subdominant, orbital-lattice interactions. Our results suggest that direct orbital exchange may be crucial for the physics of many orbitally active materials, including manganites, ruthenates and the iron pnictides.

It has long been believed that the prototypical orbital ordering material KCuF$_3$ exhibits Kugel–Khomskii (KK)-type orbital order[1], which causes Jahn–Teller distortions of the CuF$_6$ octahedra, at temperatures below $T_{JT} \sim 800$ K (refs 4–7). However, several properties of KCuF$_3$ have never fully been explained by the KK model. First, whereas the orbitals order at temperatures of the order of 800 K, the spins order below a much lower Néel temperature, $T_N = 40$ K (ref. 5). The KK model can account for, at most, a factor of 10 difference between these two energy scales[1,8]. Second, whereas the KK model correctly accounts for the relative signs of the in-plane and out-of-plane spin superexchange, it does not explain their disparate magnitudes[8–11]. Finally, several authors have recently reported unexplained structural fluctuations associated with the F$^-$ ions at temperatures far below T_{JT}, where, according to the KK model, structural fluctuations should be frozen out[12–15].

To gain further insight into these discrepancies, we carried out Raman scattering, as well as hard- and soft-X-ray scattering, measurements of the lattice and magnetic degrees of freedom in KCuF$_3$ (see Methods). At $T = 10$ K the Raman spectrum (Fig. 1) exhibits several modes associated with vibrations of the F$^-$ ions, with A$_{1g}$, B$_{1g}$ and E$_g$ symmetry, consistent with previous studies[16].
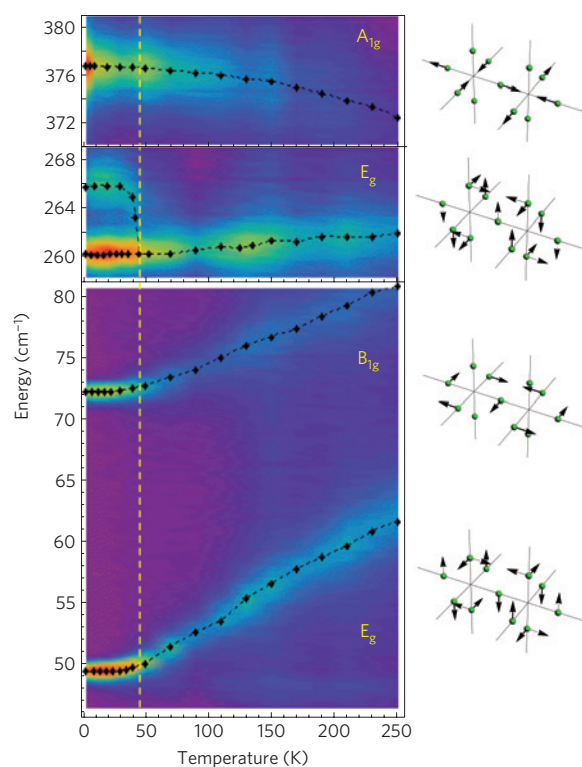
Figure 1 | Temperature dependence of the Raman-active phonons in KCuF$_3$, and their corresponding eigenvectors showing displacements of the F$^-$ ions[16]. The temperature dependence of the A$_{1g}$-symmetry phonon near 377 cm^{-1} (top panel) is consistent with normal anharmonic effects. However, the E$_g$-symmetry phonon near 50 cm^{-1} and the B$_{1g}$-symmetry phonon near 72 cm^{-1} (bottom panel) exhibit a roughly tenfold decrease in linewidth (FWHM), and a 20% and 10% decrease in energy, respectively, with decreasing temperature. At $T = 50$ K—just above the Néel temperature—the frequencies stabilize and the 260 cm^{-1} E$_g$ mode (middle panel) splits into two singly degenerate modes at 260 cm^{-1} and 266 cm^{-1}. This behaviour is consistent with a tetragonal-to-orthorhombic phase transition associated with rotations of the CuF$_6$ octahedra.

[1]Department of Physics and Frederick Seitz Materials Research Laboratory, University of Illinois, Urbana, Illinois 61801, USA, [2]Institute for Condensed Matter Theory, University of Illinois at Urbana-Champaign, Urbana, Illinois 61801, USA, [3]Cornell High Energy Synchrotron Source, Cornell University, Ithaca, New York 14850, USA, [4]Advanced Photon Source, Argonne National Laboratory, Argonne, Illinois 60439, USA, [5]National University of Singapore, 21 Lower Kent Ridge Road, 119077, Singapore. †Present address: Department of Physical Sciences, IISER-Kolkata, Mohanpur Campus, West Bengal 741252, India. *e-mail: slcooper@illinois.edu; abbamonte@mrl.illinois.edu.

We have found that several of these modes exhibit anomalous temperature dependencies. Whereas the A_{1g} mode behaves in a manner expected from normal anharmonic effects, shifting to higher frequency with decreasing temperature, the B_{1g} and E_g modes soften anomalously in the range $50\,\mathrm{K} < T < 300\,\mathrm{K}$ (Fig. 1, middle and lower panels). At $T = 50\,\mathrm{K}$—just above the Néel temperature—the frequencies of the modes stabilize and the higher E_g mode splits into two, distinct, non-degenerate modes (Fig. 1). These observations indicate a reduction in crystal symmetry from tetragonal to orthorhombic, and may be understood as the stabilization of GdFeO$_3$-type rotations of the CuF$_6$ octahedra at $T_R = 50\,\mathrm{K}$. This interpretation is further supported by X-ray measurements, described below. The anomalous structural fluctuations observed in refs 12–15 can, then, be understood as arising from critical, precursor fluctuations of this transition. The close coincidence of T_R and T_N suggests that freezing in of CuF$_6$ rotations contributes to the stabilization of Néel spin order.

To explain the relationship between octahedral rotations and Néel order in KCuF$_3$, we suggest a refined version of the KK model. Its main new ingredient is a direct-orbital exchange term proposed in ref. 3, described by the Hamiltonian

$$H_{\tau\tau} = \sum_{\langle ij \rangle} \sum_{\alpha=a,b,c} J_1^\alpha \tau_i^\alpha \tau_j^\alpha \qquad (1)$$

where the hole orbital on site i, which lies in $3d_{3z^2-r^2}$ or $3d_{x^2-y^2}$ orbitals, is described by pseudospin operators τ_i^a, τ_i^b and τ_i^c (see Supplementary Information; ref. 17), and J_1^α is the nearest-neighbour orbital coupling along the a, b and c directions. Equation (1) was argued[3] to be the dominant coupling between orbitals in a charge-transfer insulator, and can arise from either on-ligand interactions or cooperative Jahn–Teller distortions[18,19].

The orbital–spin interactions are described by the usual KK superexchange Hamiltonian,

$$
\begin{aligned}
H_{\tau S} = & \sum_{\langle ij \rangle} \sum_{\alpha=a,b,c} J_2^\alpha \left[4(\mathbf{S}_i \cdot \mathbf{S}_j)\left(\tau_i^\alpha - \frac{1}{2}\right)\left(\tau_j^\alpha - \frac{1}{2}\right) \right. \\
& + \left(\tau_i^\alpha + \frac{1}{2}\right)\left(\tau_j^\alpha + \frac{1}{2}\right) - 1 \Bigg] \\
& + \eta \sum_{\langle ij \rangle} \sum_{\alpha=a,b,c} J_2^\alpha \left[(\mathbf{S}_i \cdot \mathbf{S}_j)(\tau_i^\alpha + \tau_j^\alpha - 1) \right. \\
& + \frac{1}{2}\left(\tau_i^\alpha - \frac{1}{2}\right)\left(\tau_j^\alpha - \frac{1}{2}\right) + \frac{3}{2}\left(\tau_i^\alpha \tau_j^\alpha - \frac{1}{4}\right) \Bigg] \qquad (2)
\end{aligned}
$$

where $\mathbf{S}_i$ denotes the true electron spin[1]. Following ref. 17, a Hund's rule term has been included, where the parameter $\eta = J_H/U \ll 1$ is the ratio of the Hund coupling J_H to the Hubbard U parameter for the d electrons. Crucially, as suggested in ref. 3, we assume $J_1 \gg J_2$, that is, that the orbital–spin interactions play a sub-dominant role and mainly determine the impact of orbital physics on the development of magnetic order[1,3,17]. This assumption is justified by the different influence of Jahn–Teller distortions on these parameters, discussed below.

Finally, we include a coupling of the orbitals and spins to the orthorhombic rotations of the octahedra,

$$H_{OR} = -\mu \sum_{\langle ij \rangle} \sum_{\alpha=a,b} J_2^\alpha (\mathbf{S}_i \cdot \mathbf{S}_j)\left(\tau_i^\alpha - \frac{1}{2}\right)\left(\tau_j^\alpha - \frac{1}{2}\right) |\mathbf{Q}_{ij}|^2 \qquad (3)$$

where the dynamical variables $\mathbf{Q}_{ij}$ describe fluctuations in the positions of the F$^-$ ion transverse to the line connecting adjacent in-plane Cu sites i and j, and μ describes the coupling between the orbital-spin fluctuations and the octahedral rotations. By symmetry, H_{OR} depends on $|\mathbf{Q}_{ij}|^2$, which we shall see favours the formation of a glassy state at low temperatures. For completeness, we also include a weak, tetragonal crystal-field term, $H_{CF} = \lambda_{CF} \sum_i \tau_i^z$, with the crystal-field coupling $\lambda_{CF} \ll J_1$. Our complete Hamiltonian is the sum of the four terms $H_{eff} = H_{\tau\tau} + H_{\tau S} + H_{OR} + H_{CF}$. To analyse this model we take the usual variational approach[1,11,17], optimizing the energy with respect to a hybrid orbital wavefunction, $|i\sigma\rangle = \cos(\theta_i)|iz\sigma\rangle + \sin(\theta_i)|ix\sigma\rangle$, which represents the orbital configuration on lattice site i. Here, $|iz\sigma\rangle$ represents a $d_{3z^2-r^2}$ orbital, and $|ix\sigma\rangle$ a $d_{x^2-y^2}$ orbital, with spin σ and mixing angle θ_i as the variational parameters. The sign of θ_i is taken to alternate between the two sublattices, ensuring that the variational wavefunction has the appropriate space-group symmetry.

In our model, in the high-temperature phase ($T \gg 800\,\mathrm{K}$) the system is cubic, all coupling constants are isotropic and the physics is governed by the highest energy scale, $H_{\tau\tau}$. As the temperature is lowered, the system undergoes a transition at $T_{JT} \sim 800\,\mathrm{K}$ into a phase with cooperative Jahn–Teller distortions and orbital order, characterized by a mixing angle, $\theta \approx \pi/4$, that minimizes $H_{\tau\tau}$. We note that, in our model, this mixing angle depends only on the existence of a J_1 term regardless of the microscopic geometry of the Jahn–Teller distortion. Despite caveats about the relationship between the orbital state and the geometry of Jahn–Teller distortions[20], this result suggests that the octahedra exhibit three—rather than just two—distinct bond lengths, in agreement with the known structure[4,6].

In the intermediate-temperature regime ($50\,\mathrm{K} < T < 800\,\mathrm{K}$), according to our model, the system resides in a free-energy minimum corresponding to the Jahn–Teller distorted state. To understand what happens at lower energy scales, it is necessary to use effective coupling constants that describe small excursions around this minimum, that is, that apply to the Jahn–Teller-distorted structure. The primary effect of the Jahn–Teller distortion is to introduce anisotropy in the exchange parameters J_1 and J_2. The anisotropy in J_2, which arises purely from superexchange and depends exponentially on the bond lengths, should be more pronounced than that in J_1, which has a crystal-field component and power-law dependence. We therefore anticipate that $J_2^c > J_2^a (=J_2^b)$ and $J_1^a = J_1^b \approx J_1^c$.

Surprisingly, minimizing H_{eff} reveals a ground state that is nearly degenerate. Two distinct hybrid orbital states—called $|HO_1\rangle$ and $|HO_2\rangle$—were found, which exhibit G-type and A-type order, respectively (see Supplementary Information). Both of these states are characterized by mixing angles close to $\theta \approx \pi/4$ (see Fig. 2a,b), and their energies are separated by the smallest couplings in the problem:

$$\Delta E = E_{HO_1} - E_{HO_2} \approx \left(\eta - \frac{1}{4}\right)J_2^{a/b} + \frac{\eta}{4}J_2^c + \frac{\mu}{16}|\mathbf{Q}|^2 \qquad (4)$$

Note that, in our model, the KK ground state[1], characterized by a mixing angle $\theta = \pi/6$ and corresponding to alternating $3d_{x^2-z^2}$ and $3d_{y^2-z^2}$ orbitals, is higher than $|HO_1\rangle$ and $|HO_2\rangle$ by an energy of the order of $3J_1/8$.

The near degeneracy of $|HO_1\rangle$ and $|HO_2\rangle$ explains the existence of both the extended fluctuational regime and the second structural transition in KCuF$_3$. For illustration, we choose the parameter values $J_1^a = 600\,\mathrm{K}$, $J_1^c = 630\,\mathrm{K}$, $J_2^c = 200\,\mathrm{K}$, $J_2^{a/b} = 30\,\mathrm{K}$, $\lambda_{CF} = 50\,\mathrm{K}$ and $\eta = 0.1$ (see refs 1,9–11,17). These choices reflect the dominant role of J_1, which arises partly from lattice effects, as well as the expected larger anisotropy in J_2. For these values, we find the
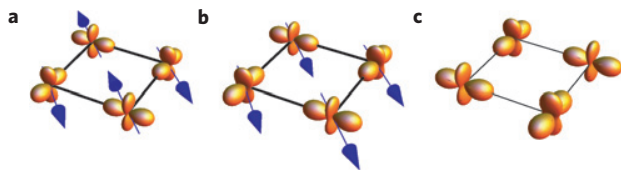
Figure 2 | Nearly degenerate hybrid orbital states. a, $|HO_1\rangle$, which corresponds to a mixing angle of $\theta = 0.244\pi$; **b,** $|HO_2\rangle$, whose mixing angle is $\theta = 0.256\pi$. The blue arrows indicate the spin direction on the Cu site (mixing angles have been exaggerated slightly for clarity). These two states are thermally occupied in the intermediate-temperature regime. The $|HO_2\rangle$ state is stabilized by the low-temperature, orthorhombic distortion. **c,** Difference between the two hybrid orbital states, $|HO_1\rangle - |HO_2\rangle$, which illustrates the symmetry of the fluctuations.

energy difference between $|HO_1\rangle$ and $|HO_2\rangle$ to be of the order of a few Kelvin. Hence, throughout the intermediate-temperature regime (50 K < T < 800 K), the system undergoes rapid fluctuations between the two hybrid orbital configurations. Each is coupled to the octahedral rotations through equation (3), resulting in the extended regime of dynamic, orthorhombic distortions reported in several studies[6,14,15].

Although the size of the orbital fluctuations (as reflected in Fig. 2) is small, in our model their consequences for the in-plane magnetic order are severe. As $|HO_1\rangle$ and $|HO_2\rangle$ have opposite in-plane spin exchange, even small orbital fluctuations disrupt the in-plane magnetic order[17]. This is consistent with the experimental observation that, in the intermediate-temperature regime, the in-plane spin correlations are shorter ranged than those along the c axis.

At the lower structural transition, $T_R = 50$ K, the orthorhombic fluctuations freeze into a static pattern of GdFeO$_3$-type rotations of the CuF$_6$ octahedra, resulting in a non-zero value of the variable $|\mathbf{Q}|^2$. This distortion, in accordance with equation (4), lifts the near-degeneracy, lowering the energy of the $|HO_2\rangle$ state when compared with $|HO_1\rangle$, resulting in A-type antiferromagnetic order.

The emergence of in-plane spin correlations, in our model, has pronounced effects on the stiffness of the lattice, explaining the anomalous phonon shifts observed in KCuF$_3$ (see Fig. 1). According to equation (3), aligned neighbouring spins cause a

softening of the lattice, whereas anti-aligned neighbours cause a hardening. This implies that, as the ferromagnetic (A-type) in-plane correlations develop with decreasing temperature, the spring constant decreases, leading to the phonon softening shown in Fig. 1 (see Supplementary Information).

Our model also provides some explanation for the extreme anisotropy in the spin exchange, Γ, in KCuF$_3$, which neutron-scattering experiments have suggested is as large as $\Gamma^c/\Gamma^{a/b} \sim -100$ below the Néel temperature[9,10]. Using our parameter values, we find $\Gamma^c = 180$ K and $\Gamma^{a/b}_{HO_2} = -2$ K, or $\Gamma^c/\Gamma^{a/b}_{HO_2} = -90$ (see Supplementary Information). Some of this anisotropy arises from our chosen anisotropy $J^c_2/J^a_2 = 6.67$, which is expected from the symmetry of the Jahn–Teller distortion. We emphasize, however, that our orbital pattern provides the correct sign of $\Gamma^c/\Gamma^{a/b}_{HO_2}$, and further amplifies its magnitude above $J^c_2/J^{a/b}_2$ by a factor of 13.5. This amplification is an outcome of the small value of the Cu^{2+} Hund parameter, η, and the small in-plane overlap of our orbitals (Fig. 2b) due to their staggered arrangement.

To confirm the relationship between tilting of the CuF$_6$ octahedra and the magnetic ordering transition, we also studied KCuF$_3$ with conventional and magnetic X-ray scattering (see Methods). Magnetic-scattering studies, summarized in Fig. 3a, show that long-ranged, A-type antiferromagnetic order sets in at $T_N = 40$ K, in agreement with previous studies[5,9,10]. Above T_N, diffuse magnetic scattering is observed, which arises from critical fluctuations in the magnetic order. The momentum linewidth is highly anisotropic, indicating quasi-one-dimensional magnetism, as has been observed above T_N (ref. 10). The correlation length in all three directions diverges simultaneously, indicating a single, three-dimensional Néel transition.

Hard-X-ray measurements are summarized in Fig. 3b, showing scans through the (1,0,5) Bragg position, which corresponds to the wave vector of both the orbital order and the CuF$_6$ rotations, and is symmetry equivalent to the orbital reflections studied in ref. 7. The (1,0,5) reflection is present at room temperature, consistent with the existence of Jahn–Teller-distorted octahedra at $T < 800$ K. As the temperature is lowered the intensity of this reflection increases, reaching a maximum at $T \sim 100$ K, that is, in the middle of the fluctuational regime identified in Raman measurements (Fig. 1). This observation supports the interpretation that the fluctuations arise from CuF$_6$ rotations, which amplify the (1,0,5) structure
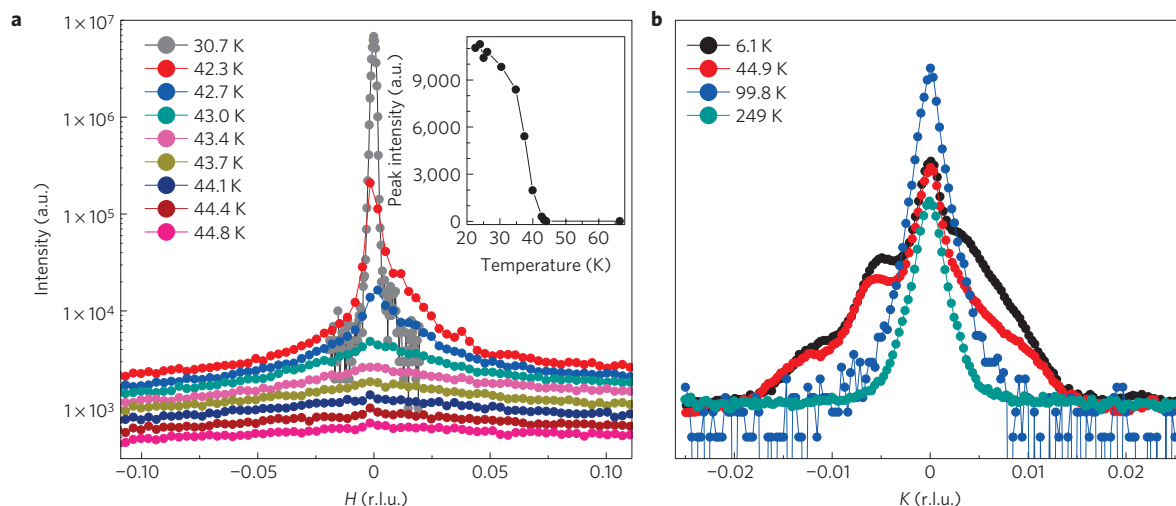
Figure 3 | Magnetic and structural X-ray scattering from KCuF$_3$. a, Resonant scattering at the Cu L$_{3/2}$ edge of the (0,0,1) reflection, which is an order parameter for A-type antiferromagnetism. Critical magnetic fluctuations, visible above T_N, reveal highly anisotropic spin correlations in the fluctuating regime. Inset: Temperature dependence of the magnetic order parameter below T_N. **b,** Non-resonant scattering at 8.8 keV, showing the temperature dependence of the (1,0,5) Bragg reflection, which serves as an order parameter for both the orbital ordering and the GdFeO$_3$-type rotations of the CuF$_6$ octahedra.

factor. Finally, for $T < T_N$, the (1,0,5) reflection abruptly drops in intensity and acquires a series of diffuse sidebands that exhibit hysteresis when cycling the temperature through T_N. This suggests that the CuF_6 rotations become static below T_N, but are glassy and short-range ordered.

Such glassy order is a natural outcome of equation (3). As the spin correlations couple to the magnitude, $|\mathbf{Q}|^2$, and are insensitive to the sign of $\mathbf{Q}$, the free-energy cost of forming domain walls in the CuF_6 tilt pattern is small. We expect, therefore, the magnetically ordered state to be associated with a large number of nearly degenerate configurations of tilt patterns, resulting in glassy behaviour.

Overall, our model suggests a picture of $KCuF_3$ in which the orbital order occurs not through a single transition near 800 K, as is commonly believed, but in two stages: the higher-temperature transition reduces the manifold of available orbital states, but leaves a pair of nearly degenerate (to within a few Kelvin) hybrid states that have similar orbital configurations but very different in-plane spin configurations. The near degeneracy of these states results in a large temperature range of structural and in-plane spin fluctuations, as well as anisotropy in spin correlation lengths. The lower structural transition corresponds to a freezing of the octahedral rotations, which splits the hybrid orbital states, completing the ordering of the orbitals and stabilizing A-type spin order.

If correct, our result indicates that direct, orbital–orbital exchange—the key new ingredient in our model—may be crucial to the physics of many orbitally active materials, including manganites[2], ruthenates[21,22] and the iron pnictides[23]. One curious consequence of equation (1) is that the orbital pattern in Fig. 2 differs somewhat from the KK pattern; such deviations have also been observed in some[24], though not all[19], *ab initio* calculations. The discrepancies probably originate in the different ways in which these approaches treat the interactions on, and dynamical motions of, the F^- ligands.

Methods

The $KCuF_3$ single crystals were grown from solution by techniques described previously[25]. The crystals selected were screened with X-ray measurements and consisted of a >90% volume fraction of polytype a.

Raman scattering measurements were made in a variable-temperature, continuous-flow cryostat using the 6,471 Å line from a Kr laser. An incident power of ~10 mW and ~50 µm spot size was used to minimize laser heating. The spectra were analysed with a modified subtractive triple-stage spectrometer using a liquid-nitrogen-cooled CCD (charge-coupled device) detector.

Soft-X-ray magnetic scattering measurements were conducted at the Cu $L_{3/2}$ edge at beamline X1B at the National Synchrotron Light Source (NSLS). Hard-X-ray measurements were made at Sectors 4 (CARS) and 15 at the Advanced Photon Source and C Line at the Cornell High Energy Synchrotron Source (CHESS). We denote momenta in terms of Miller indices, that is, (H, K, L) indicates a momentum transfer $\mathbf{q} = (2\pi H/a, 2\pi K/b, 2\pi L/c)$, where $a = b = 5.85$ Å and $c = 7.82$ Å.

References

1. Kugel, K. I. & Khomskii, D. I. Crystal structure and magnetic properties of substances with orbital degeneracy. *Sov. Phys.-JETP* **37,** 725–730 (1973).
2. Tokura, Y. & Nagaosa, N. Orbital physics in transition-metal oxides. *Science* **21,** 462–468 (2000).
3. Mostovoy, M. V. & Khomskii, D. I. Orbital ordering in charge transfer insulators. *Phys. Rev. Lett.* **92,** 167201 (2004).
4. Okazaki, A. & Suemune, Y. The crystal structure of $KCuF_3$. *J. Phys. Soc. Jpn* **16,** 176–183 (1961).
5. Hutchings, M. T., Samuelsen, E. J., Shirane, G. & Hirakawa, K. Neutron diffraction determination of the antiferromagnetic structure of $KCuF_3$. *Phys. Rev.* **188,** 919–923 (1969).
6. Hidaka, M., Eguchi, T. & Yamada, I. New superlattice crystal structure in $KCuF_3$ revealed by x-ray diffraction experiments. *J. Phys. Soc. Jpn* **67,** 2488–2494 (1998).
7. Paolasini, L., Caciuffo, R., Sollier, A., Ghigna, P. & Altarelli, M. Coupling between spin and orbital degrees of freedom in $KCuF_3$. *Phys. Rev. Lett.* **88,** 106403 (2002).
8. Polinger, V. *The Jahn–Teller-Effect: Fundamentals and Implications for Physics and Chemistry* 685–725 (Springer, 2009).
9. Sajita, S. K., Axe, J. D., Shirane, G., Yoshizawa, H. & Hirakawa, K. Neutron scattering study of spin waves in one-dimensional antiferromagnet $KCuF_3$. *Phys. Rev. B* **21,** 2001–2007 (1980).
10. Lake, B., Tennant, D. A., Frost, C. D. & Nagler, S. E. Quantum criticality and universal scaling of a quantum antiferromagnet. *Nature Mater.* **4,** 329–334 (2005).
11. Oleś, A. M., Khaliullin, G., Horsch, P. & Feiner, L. F. Fingerprints of spin-orbital physics in cubic Mott insulators: Magnetic exchange interaction and optical spectral weights. *Phys. Rev. B* **72,** 214431 (2005).
12. Mazzoli, C., Allodi, G., De Renzi, R., Guidi, G. & Ghigna, P. Zeeman perturbed nuclear quadrupole resonance investigation of orbitally ordered $KCuF_3$. *J. Magn. Magn. Mater.* **242,** 935–938 (2002).
13. Yamada, I. & Kato, N. Multi-sublattice magnetic structure of $KCuF_3$ caused by the antiferromagnetic exchange interaction: Antiferromagnetic resonance measurements. *J. Phys. Soc. Jpn* **63,** 289–297 (1994).
14. Eremin, M. V. *et al.* Dynamical Dzyaloshinsky–Moriya interaction in $KCuF_3$. *Phys. Rev. Lett.* **101,** 147601 (2008).
15. Deisenhofer, J. *et al.* Optical evidence for symmetry changes above the Néel transition of $KCuF_3$. *Phys. Rev. Lett.* **101,** 157406 (2008).
16. Ueda, T., Sugawara, K., Kondo, T. & Yamada, I. Raman scattering studies of phonons in $KCuF_3$. *Sol. St. Commun.* **80,** 801–805 (1991).
17. Feiner, L. F., Oles, A. M. & Zaanen, J. Quantum melting of magnetic order due to orbital fluctuations. *Phys. Rev. Lett.* **78,** 2799–2802 (1997).
18. Lin, C. & Millis, A. J. Theoretical description of pseudocubic manganites. *Phys. Rev. B* **78,** 174419 (2008).
19. Pavarini, E., Koch, E. & Lichtenstein, A. I. Mechanism for orbital ordering in $KCuF_3$. *Phys. Rev. Lett.* **101,** 266405 (2008).
20. Sboychakov, A. O., Kugel, K. I., Rakhmanov, A. L. & Khomskii, D. I. Relationship between orbital structure and lattice distortions in Jahn–Teller systems. *Phys. Rev. B* **83,** 205123 (2011).
21. Snow, C. S. *et al.* Pressure-tuned collapse of the Mott-like state in $Ca_{n+1}Ru_nO_{3n+1}$ ($n = 1, 2$): Raman spectroscopic studies. *Phys. Rev. Lett.* **89,** 226401 (2002).
22. Fang, Z., Terakura, K. & Nagaosa, N. Orbital physics in ruthenates: First-principles studies. *New J. Phys.* **7,** 66 (2005).
23. Kruger, F., Kumar, S., Zaanen, J. & van den Brink, J. Spin-orbital frustrations and anomalous metallic state in iron-pnictide superconductors. *Phys. Rev. B* **79,** 054504 (2009).
24. Binggelli, N. & Altarelli, M. Orbital ordering, Jahn–Teller distortion, and resonant x-ray scattering in $KCuF_3$. *Phys. Rev. B* **70,** 085117 (2004).
25. Hirakawa, K. & Kurogi, Y. One-dimensional antiferromagnetic properties of $KCuF_3$. *Suppl. Prog. Theor. Phys.* **46,** 147–161 (1970).

Author contributions

S.Y. and J.C.T.L. grew the crystals. S.Y. carried out Raman experiments. J.C.T.L., Y.I.J., S.S., Y.F., Y.G., A.R. and K.F. carried out the X-ray experiments. S.L., P.M.G. and P.A. developed the model. P.A. and S.L.C. wrote the paper.